

Master Thesis

Load Sharing - Obstacle Avoidance and Admittance Control on a Mobile Manipulator

Spring Term 2018

Supervised by:

Professor Jonathan Kelly
Professor Marco Hutter

Author:

Tobias Ulrich

Declaration of Originality

I hereby declare that the written work I have submitted entitled

Your Project Title

is original work which I alone have authored and which is written in my own words.¹

Author(s)

Tobias	Ulrich
--------	--------

Student supervisor(s)

Jonathan	Kelly
----------	-------

Supervising lecturer

Marco	Hutter
-------	--------

With the signature I declare that I have been informed regarding normal academic citation rules and that I have read and understood the information on ‘Citation etiquette’ (<https://www.ethz.ch/content/dam/ethz/main/education/rechtliches-abschluesse/leistungskontrollen/plagiarism-citationetiquette.pdf>). The citation conventions usual to the discipline in question here have been respected.

The above written work may be tested electronically for plagiarism.

Place and date

Signature

¹Co-authored work: The signatures of all authors are required. Each signature attests to the originality of the entire piece of written work in its final form.

Intellectual Property Agreement

The student acted under the supervision of Prof. Hutter and contributed to research of his group. Research results of students outside the scope of an employment contract with ETH Zurich belong to the students themselves. The results of the student within the present thesis shall be exploited by ETH Zurich, possibly together with results of other contributors in the same field. To facilitate and to enable a common exploitation of all combined research results, the student hereby assigns his rights to the research results to ETH Zurich. In exchange, the student shall be treated like an employee of ETH Zurich with respect to any income generated due to the research results.

This agreement regulates the rights to the created research results.

1. Intellectual Property Rights

1. The student assigns his/her rights to the research results, including inventions and works protected by copyright, but not including his moral rights ("Urheberpersönlichkeitsrechte"), to ETH Zurich. Herewith, he cedes, in particular, all rights for commercial exploitations of research results to ETH Zurich. He is doing this voluntarily and with full awareness, in order to facilitate the commercial exploitation of the created Research Results. The student's moral rights ("Urheberpersönlichkeitsrechte") shall not be affected by this assignment.
2. In exchange, the student will be compensated by ETH Zurich in the case of income through the commercial exploitation of research results. Compensation will be made as if the student was an employee of ETH Zurich and according to the guidelines "Richtlinien für die wirtschaftliche Verwertung von Forschungsergebnissen der ETH Zürich".
3. The student agrees to keep all research results confidential. This obligation to confidentiality shall persist until he or she is informed by ETH Zurich that the intellectual property rights to the research results have been protected through patent applications or other adequate measures or that no protection is sought, but not longer than 12 months after the collaborator has signed this agreement.
4. If a patent application is filed for an invention based on the research results, the student will duly provide all necessary signatures. He/she also agrees to be available whenever his aid is necessary in the course of the patent application process, e.g. to respond to questions of patent examiners or the like.

2. Settlement of Disagreements

Should disagreements arise out between the parties, the parties will make an effort to settle them between them in good faith. In case of failure of these agreements, Swiss Law shall be applied and the Courts of Zurich shall have exclusive jurisdiction.

Place and date

Signature

Contents

Preface	v
Abstract	vii
Symbols	ix
1 Introduction	1
2 Related Work	3
3 Mobile Manipulator	4
3.1 Ridgeback	4
3.2 Universal Robot 10	4
3.3 Gripper	6
3.4 Force-Torque Sensor	6
4 Admittance Control	8
5 Obstacle Avoidance	9
5.1 Local Planners	9
5.1.1 Velocity Obstacles	9
5.1.2 Dynamic Window Approach	10
5.1.3 Potential Fields	10
6 Implementation	12
6.1 Admittance Control and Obstacle Avoidance Fusion	12
6.1.1 Parameters	12
6.1.2 Costmap	12
6.2 Inverse Kinematics	14
7 Results	15
7.1 Admittance Control Performance	15
7.1.1 Force Excitement in X	17
7.1.2 Force Excitement in Y	17
7.1.3 Force Excitement in Theta	17
7.2 Obstacle Avoidance Performance	17
7.2.1 Frontal Obstacle	17
7.2.2 Corridor	17
7.3 Real World Scenarios Performance	17
7.3.1 Corner	17
7.3.2 Double Slalom	18
7.3.3 Triple Slalom	18
7.3.4 Cluttered Space 1	18

7.3.5	Cluttered Space 2	18
8	Conclusions	19
9	Einige wichtige Hinweise zum Arbeiten mit L^AT_EX	20
9.1	Gliederungen	20
9.2	Referenzen und Verweise	20
9.3	Aufzählungen	20
9.4	Erstellen einer Tabelle	21
9.5	Einbinden einer Grafik	22
9.6	Mathematische Formeln	22
9.7	Weitere nützliche Befehle	23
	Bibliography	25
	A Code	27
	B Datasheets	29

Preface

Bla bla ...

Abstract

Hier kommt der Abstact hin ...

Symbols

Symbols

ϕ, θ, ψ	roll, pitch and yaw angle
b	gyroscope bias
Ω_m	3-axis gyroscope measurement

Indices

x	x axis
y	y axis

Acronyms and Abbreviations

ETH	Eidgenössische Technische Hochschule
EKF	Extended Kalman Filter
IMU	Inertial Measurement Unit
UAV	Unmanned Aerial Vehicle
UKF	Unscented Kalman Filter

Chapter 1

Introduction

Hier kommt die Einleitung

Chapter 2

Related Work

As with many fields in robotics, Human Robot Interaction (HRI) has seen a lot of development in the last twenty years. Research has come from teleoperated assistive robots to dynamically and independently collaborating robots. This advancement is expressed by the newly joined terms in literature to differentiate between types of interaction and level of autonomy for the robot.

Chapter 3

Mobile Manipulator

We conduct our research on a mobile manipulator, lovingly called the *Thing*. It is composed of four main components, on which we elaborate in detail in this chapter. The first is the Ridgeback, a omnidirectional robot platform , followed by the UR10, a six degrees of freedom (DOF) robot arm with a three finger gripper as it's end effector. A force torque sensor is embedded in the wrist of the gripper. The whole manipulator is an out of the box system assembled by Clearpath, which collaborates with Universal Robots and Robotiq and mounts the parts on the platform in house.

3.1 Ridgeback

Table 3.1: Clearpath Ridgeback Specifications

Length	960 mm
Width	793 mm
Height	296 mm
Weight	135 kg
Maximum payload	100 kg
Maximum velocity	1.1 m/s
Average power consumption	800 W

The ridgeback is an omnidirectional robot platform designed by Clearpath for indoor movement and payload carrying tasks, such as autonomous warehousing for example. It is a fully integrated system with sensors, actuation and control and features a native ROS interface. Onboard sensors consist of an IMU and a front facing Hokuyo laser range finder (LIDAR) and a Kinect2 camera and wheel odometry. Optionally, a second, rear facing LIDAR can be mounted for full 360 ° coverage. The broad range of sensors, it's flexibility and low drift in odometry makes the Ridgeback a suitable and popular platform for research in controlled indoor environments. Additionally, the Ridgeback houses the onboard computer that runs the low-level drivers of all the elements of the manipulator. On top thereof, there is a high-level driver that ensures accord and offers a ROS interface for the user to connect to.

3.2 Universal Robot 10

The UR10 is an collaborative industrial robot arm by Universal Robots. It has six rotary joints with gives it six DOF and can support payloads up to 10 kg. Together



Figure 3.1: Clearpath Ridgeback



Figure 3.2: Universal Robot 10



Figure 3.3: Robotiq 3-Finger Adaptive Robot Gripper

with it's little brother the UR5, it is widely regarded as the standard manipulator within robotics research. Hence, extensive platform and software integration resources are available and ROS is supported out of the box.

Table 3.2: Universal Robot 10 Specifications

Reach	1300 mm
Weight	1.5 kg
Repeatability	0.1 mm
Maximum payload	10 kg
Maximum tool velocity	1 m/s
Degrees of freedom	6 rotating joints
Average power consumption	W

3.3 Gripper

Table 3.3: Robotiq 3-Finger Adaptive Robot Gripper Specifications

Weight	2.3 kg
Repeatability	0.1 mm
Maximum payload (encompassing grip)	10 kg
Gripper opening	0 to 155 mm
Object diameter for encompassing	20 to 155 mm
Grip force	30 to 70 N
Minimum power consumption	4.1 W
Peak power (at maximum gripping force)	36 W

3.4 Force-Torque Sensor

labelsec:ft300



Figure 3.4: Robotiq FT 300 Force Torque Sensor

Table 3.4: Robotiq FT 300 Force Torque Sensor Specifications

Measuring range	
Force F_x, F_y, F_z	$\pm 300 \text{ N}$
Moment M_x, M_y, M_z	$\pm 30 \text{ Nm}$
Signal noise¹	
Force F_x, F_y, F_z	0.1 N / 1 N
Moment M_x, M_y	0.05 Nm / 0.02 Nm
Moment M_z	0.03 Nm / 0.01 Nm
Data output rate	100 Hz
Weight	300 g

¹ Signal noise is the standard deviation of the signal measured over a period of one second.

Chapter 4

Admittance Control

The term admittance is closely coupled to impedance [?].

The interaction between force input and motion output is modeled as a second order spring mass damper system according to Newton's second law of motion, which states that the change in momentum is equal to the sum of all forces acting on our rigid body

$$M \cdot \ddot{X} = \sum F \quad (4.1)$$

The forces in the case of a mass spring damper system are

$$\sum F = F_D + F_K + F_{ext} \quad (4.2)$$

which consists of a spring term

$$F_K = K \cdot X \quad (4.3)$$

with spring constant K , a damping term

$$F_D = D \cdot \dot{X} \quad (4.4)$$

with damping constant D and a term F_{ext} for external forces acting on the body. Replacing $\sum F$ in Equation 4.1 with Equation 4.2 and dividing by M yields the equation for a second order mass spring damper system:

$$\ddot{X} = M^{-1}(F_{ext} - D \cdot \dot{X} - K \cdot X) \quad (4.5)$$

Chapter 5

Obstacle Avoidance

Ever since robots faced the task of autonomous navigation, obstacle avoidance has been a crucial element of it. There are numerous approaches to tackle the problem, varying in degrees of foresight and influence on the path planner.

The problem can be separated into two categories, path planning around obstacles on a global scale and on a local scale. The first category bundles algorithms that take a goal position and a current position of a robot and calculate the optimal path (usually the shortest path) in between, given some objective function and a map. Since the distance to the goal is normally greater than the range of any obstacle detection sensor, these algorithms need a full map of the environment. Widely used examples are A*, Djikstra, Bit* and RRT.

In contrast, path planning on a local scale takes obstacle detection sensor information as an input and outputs commands to a drive unit, that meet the given objective, which is usually to avoid collisions and stay clear of an obstacle by a minimum distance.

A typical path planning infrastructure on a robot consists of both a global and a local planner, where the global planner outputs a path to follow to the local planner, which in terms fuses that path with online obstacle detection sensor information to ensure it is indeed collision free and deviates from it if necessary.

To find the path planning algorithm that best meets our needs, we must first examine what are the given inputs and the desired outputs of our system. As we already elaborated in chapter 1, we are working in a master-slave scenario, which means that the robot is trying to achieve the goal of its human counterpart and not its own. This manifests in the planner in such a way, that the input is the force and torque applied by the human and the robot has no global goal pose. Hence, we are inherently bound to iteratively updated goals within close proximity and there is no possibility nor need to apply global path planning techniques and we focus only on local planners in the remainder of this chapter.

5.1 Local Planners

In this chapter, we discuss a selection of common local planning methods and their feasibility for the task at hand.

5.1.1 Velocity Obstacles

Velocity Obstacles (VO) [1]

$$p_{RO} + v_R t < r_R + r_O \quad (5.1)$$

$$VO_{RO} = DTODOfillin \quad (5.2)$$

5.1.2 Dynamic Window Approach

The Dynamic Window Approach (DWA) [2] is a well-known algorithm that produces command velocities for a planar robot given vehicle dynamics and obstacle measurements. The basic assumption is that the robot moves instantaneously on circular arcs with a translational velocity v and a rotational velocity ω . Thus, the complexity is greatly simplified and calculations are performed in the 2D velocity space (v, ω) . Within this space, we compute three sets of velocity pairs, subsequently called *windows* for every iteration of the algorithm.

The *obstacle window* V_o are the measurements of any obstacles, e.g. taken by a range laser sensor and transformed from cartesian to v, ω space.

The *static window* V_s expresses the constraint velocities of the vehicle, i.e., absolute maximum and minimum velocity. As the name suggests, these parameters are usually static and do not need to be recalculated every step.

The *dynamic window* V_d are the vehicle dynamics, i.e., velocities that are physically feasible for the robot to reach within one timestep. Its size is defined by the maximal acceleration and the current velocity of the robot.

$$V_r = V_o \cap V_s \cap V_d \quad (5.3)$$

As eq. (5.3) shows, the intersection of these three sets gives us the resulting window V_r of feasible velocity pairs, that guarantee no collision with an obstacle for the next step.

A cost function is then applied to find the (v, ω) pair, that maximizes the objective within V_r . Elements are heading, distance to goal and velocity terms.

5.1.3 Potential Fields

Potential fields are also a common tool in the mobile robotics field used for path planning. A virtual potential $U(q)$ at position $q = (x, y)$ affects the robot and drives him away from any maximum, like a ball rolling downhill [3]. It can be used to attract the robot to a goal by creating a local minimum and repulsing a robot from an obstacle by creating a local maximum. The superposition of all attractive and repulsive potential fields yields the overall potential $U(q)$:

$$U(q) = U_{attr}(q) + U_{rep}(q) \quad (5.4)$$

If the potential field is differentiable, we find that the resulting virtual force $F(q)$ that acts on the robot in position q is then defined as

$$F(q) = -\nabla U(q) \quad (5.5)$$

where $\nabla U(q)$ is the gradient of the potential field

$$\nabla U(q) = \begin{pmatrix} \frac{\partial U}{\partial x} \\ \frac{\partial U}{\partial y} \end{pmatrix} \quad (5.6)$$

Analogously, by combining 5.5 and 5.4 we see that the overall force equals the sum of the attractive and repulsive forces:

$$\begin{aligned} F(q) &= F_{att}(q) + F_{rep}(q) \\ &= -\nabla U_{att}(q) - \nabla U_{rep}(q) \end{aligned} \quad (5.7)$$

An **attractive potential**, i.e. a goal is usually defined as a parabolic function

$$U_{att}(q) = \frac{1}{2} k_{att} \cdot \rho_{goal}^2(q) \quad (5.8)$$

where k_{att} is the scaling factor and ρ_{goal} is the Euclidian distance to the goal:

$$\rho_{goal} = \|q - q_{goal}\| \quad (5.9)$$

A **repulsive potential**, i.e. an obstacle is zero if a certain distance is exceeded and should rise drastically when the robot gets within close proximity of the obstacle. Hence, a common definition is

$$U_{rep}(q) = \begin{cases} \frac{1}{2} k_{rep} \cdot \left(\frac{1}{\rho(q)} - \frac{1}{\rho_0} \right)^2 & \text{if } \rho(q) \leq \rho_0 \\ 0 & \text{if } \rho(q) \geq \rho_0 \end{cases} \quad (5.10)$$

where k_{rep} is the scaling factor, ρ_0 is the distance threshold and $\rho(q)$ is the minimal distance from position q to the obstacle.

The main limitation to this approach is that it is prone to local minima, where the robot can get stuck. However, we are not working with any goals, but rather with an user input in form of a force so even if the robot is within a local minima, the user can literally pull it away from it. Furthermore, because the output of the potential field method is a force vector, we can elegantly combine it with the admittance controller, which also operates using virtual forces acting on the robot.

So we can conclude that the potential field method is most suitable for a fusion with an admittance controller and we will elaborate on our implementation in the following.

Chapter 6

Implementation

Having the potential field method selected as the desired obstacle avoidance algorithm, we are able to fuse it together with the admittance controller. Figure 6.1 shows the overall controller schematic. Firstly, we explain the functionality of the system on a higher level and dive into the specific controller blocks subsequently. Depicted on the top level are the sensor inputs, which are the readings from the *force-torque sensor* and the *LIDAR*. The force-torque sensor outputs a six-dimensional wrench F_{ext} , as described in Chapter ???. The output of the LIDAR are continuous LaserScan ROS messages [?]. Each message contains the range and intensity of every laser measurement, which is fed in the *obstacle avoidance* node. There, a costmap is created, explained in detail in Chapter ??, whose output is a planar two-dimensional wrench F_{obs} . We feed these into the *admittance control*, whose other inputs are the vehicle kinematics, namely the current pose X_{base} [?] and twist \dot{X}_{base} [?] of the ridgeback *mobile base* and the current pose X_{ee} and twist \dot{X}_{ee} of the UR10 *manipulator*. Given these inputs, we calculate the desired twist $\dot{X}_{base_{des}}$ for the mobile base and the desired twist $\dot{X}_{ee_{des}}$ for the manipulator in cartesian space, which in terms needs to be put through the *inverse kinematics* to obtain a feasible velocity \dot{q}_{ee} in joint space for the manipulator.

6.1 Admittance Control and Obstacle Avoidance Fusion

The key element of the whole algorithm is the fusion of the admittance controller, as described in Chapter ?? and the obstacle avoidance, as described in Chapter

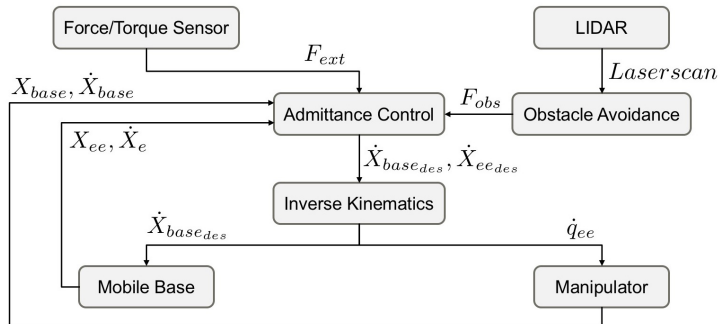


Figure 6.1: Schematic of the controller. Arrows indicate information flow between the subsets of the control architecture.

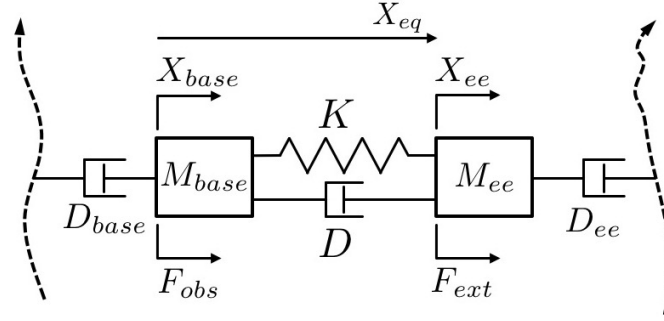


Figure 6.2: Virtual spring mass damper system with two masses. Dotted arrows represent the path of the base (left) and the arm (right) over time, connected by the spring mass damper system.

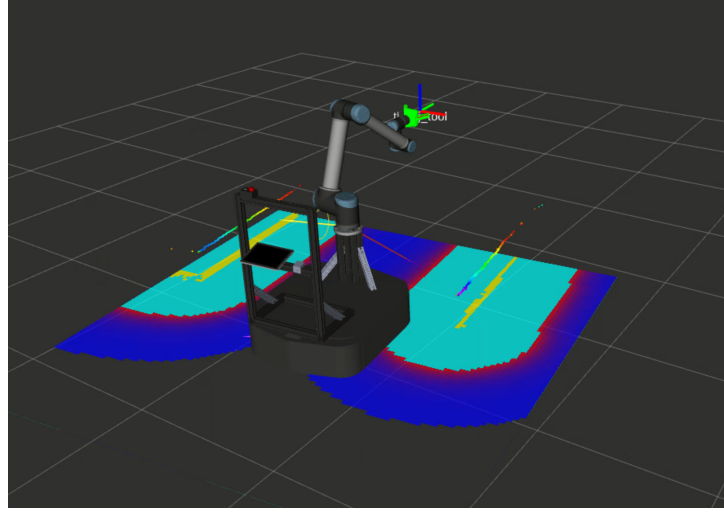


Figure 6.3: Costmap captured by the LIDAR during a test. YELLOW: Lethal, TURQUOISE: Inscribed, RED TO BLUE GRADIENT: Proximity to an obstacle, TRANSPARENT: Free space.

5.1.3. Figure 6.2 shows the coupling of base and EE.

$$M_{base} \cdot \ddot{X}_{base} = -D_{base} \cdot \dot{X}_{base} - D \cdot \dot{X}_{ee} + K \cdot X_{error} + F_{obs} \quad (6.1)$$

$$M_{ee} \cdot \ddot{X}_{ee} = -(D + D_{ee}) \cdot \dot{X}_{ee} - K \cdot X_{error} + F_{ext} \quad (6.2)$$

6.1.1 Parameters

admittance parameters

6.1.2 Costmap

Lethal dini

Inscribed sini

Obstacle proximity

Freespace

Table 6.1: Costmap Parameters.

Type	Local
Update frequency	60Hz
Publish frequency	60Hz
Width	3m
Height	3m
Resolution	0.03m
Global frame	Base link
Static map	False
Rolling window	True
Robot footprint	0.96 × 0.8m
Plugins used	Obstacles layer, inflater layer
Inflater layer cost scaling factor	10
Inflation radius	2m

6.2 Inverse Kinematics

task priority solver (parameters?)

Chapter 7

Results

We test the implementation of the previously elaborated algorithm on the Thing and list the performed tests and their results in this chapter.

7.1 Admittance Control Performance

Before any experiments on the fused algorithm can be performed, we first analyze the behaviour of the admittance controller in isolation. For this, we place the Thing in free space, i.e., in a a region with zero gradient and wegerregen the the three axes of the ridgeback seperately.

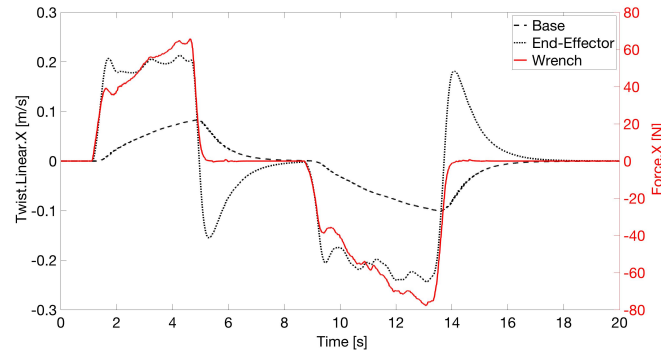
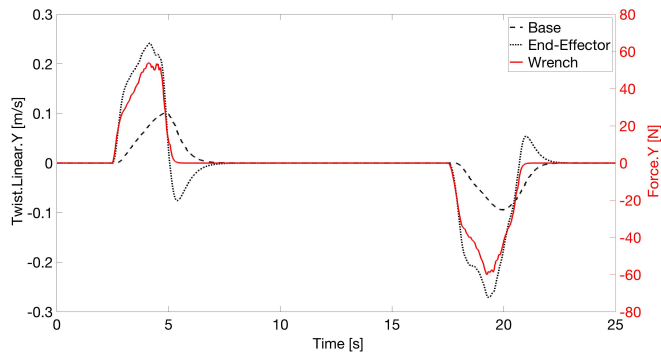
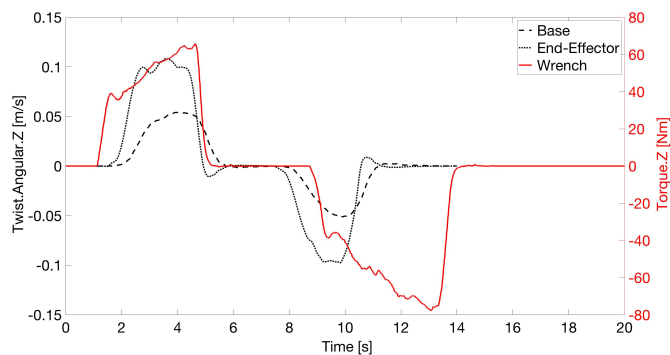
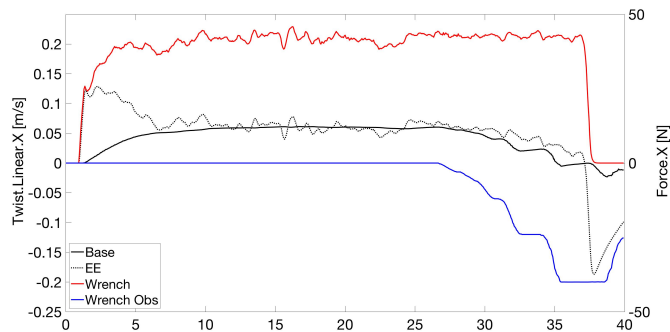


Figure 7.1: Velocity Response to Force Excitement in X

Figure 7.2: Velocity Response to Force Excitation in Y Figure 7.3: Velocity Response to Force Excitation in θ Figure 7.4: Velocity response in X axis of the robot to external and obstacle force input while being pulled in a frontal obstacle.

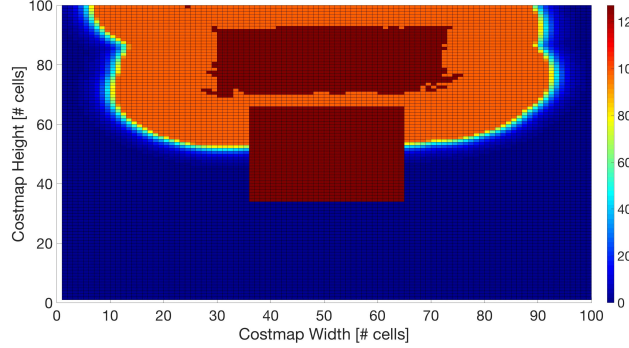


Figure 7.5: Costmap at 34s of the frontal test. Dark red indicate the obstacle and the robot base.

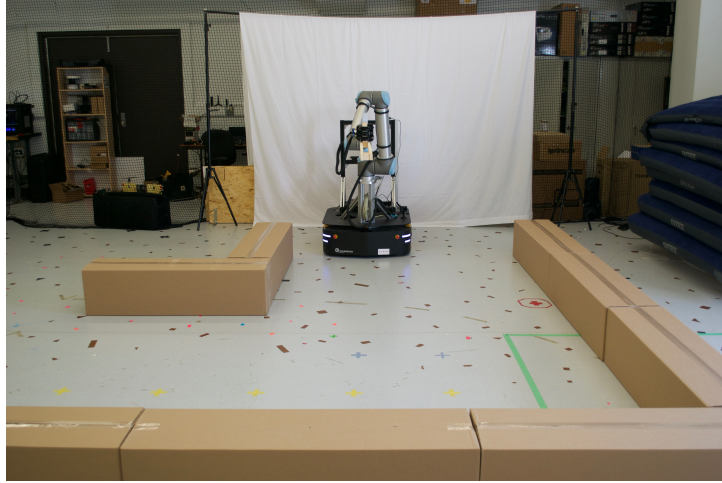


Figure 7.6: Setup of the 2m wide corner scenario.

7.1.1 Force Excitement in X

7.1.2 Force Excitement in Y

7.1.3 Force Excitement in Theta

7.2 Obstacle Avoidance Performance

7.2.1 Frontal Obstacle

7.2.2 Corridor

7.3 Real World Scenarios Performance

7.3.1 Corner

In this experiment, we asses the performance of the algorithm in a corridor with a corner. The width of corridor is 2m and we jointly carry the object through it. As we can see in fig. 7.7, there is a negative peak in the negative Y direction, which is caused by the robot drifting close the outer wall as it was making the corner. This was due to the fact, that

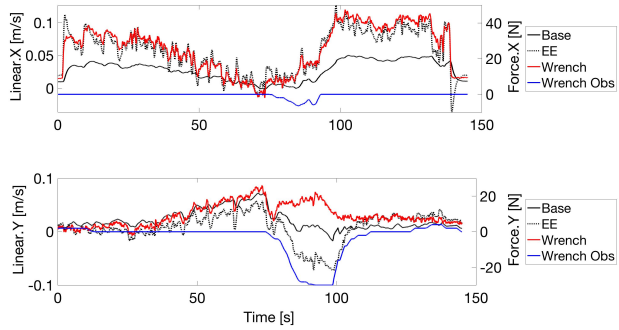


Figure 7.7: Velocity response to external and obstacle force input in 2m wide corner scenario.

7.3.2 Double Slalom

7.3.3 Triple Slalom

7.3.4 Cluttered Space 1

7.3.5 Cluttered Space 2

Chapter 8

Conclusions

Chapter 9

Einige wichtige Hinweise zum Arbeiten mit LATEX

Nachfolgend wird die Codierung einiger oft verwendeten Elemente kurz beschrieben. Das Einbinden von Bildern ist in LATEX nicht ganz unproblematisch und hängt auch stark vom verwendeten Compiler ab. Typisches Format für Bilder in LATEX ist EPS¹ oder PDF².

9.1 Gliederungen

Ein Text kann mit den Befehlen `\chapter{.}`, `\section{.}`, `\subsection{.}` und `\subsubsection{.}` gegliedert werden.

9.2 Referenzen und Verweise

Literaturreferenzen werden mit dem Befehl `\citet{.}` und `\citep{.}` erzeugt. Beispiele: ein Buch [?], ein Buch und ein Journal Paper [? ?], ein Konferenz Paper mit Erwähnung des Autors: ?].

Zur Erzeugung von Fussnoten wird der Befehl `\footnote{.}` verwendet. Auch hier ein Beispiel³.

Querverweise im Text werden mit `\label{.}` verankert und mit `\cref{.}` erzeugt. Beispiel einer Referenz auf das zweite Kapitel: chapter 9.

9.3 Aufzählungen

Folgendes Beispiel einer Aufzählung ohne Numerierung,

- Punkt 1
- Punkt 2

wurde erzeugt mit:

```
\begin{itemize}
  \item Punkt 1
  \item Punkt 2
\end{itemize}
```

¹Encapsulated Postscript

²Portable Document Format

³Bla bla.

Folgendes Beispiel einer Aufzählung mit Numerierung,

1. Punkt 1
2. Punkt 2

wurde erzeugt mit:

```
\begin{enumerate}
    \item Punkt 1
    \item Punkt 2
\end{enumerate}
```

Folgendes Beispiel einer Auflistung,

P1 Punkt 1

P2 Punkt 2

wurde erzeugt mit:

```
\begin{description}
    \item[P1] Punkt 1
    \item[P2] Punkt 2
\end{description}
```

9.4 Erstellen einer Tabelle

Ein Beispiel einer Tabelle:

Table 9.1: Daten der Fahrzyklen ECE, EUDC, NEFZ.

Kennzahl	Einheit	ECE	EUDC	NEFZ
Dauer	s	780	400	1180
Distanz	km	4.052	6.955	11.007
Durchschnittsgeschwindigkeit	km/h	18.7	62.6	33.6
Leerlaufanteil	%	36	10	27

Die Tabelle wurde erzeugt mit:

```
\begin{table}[h]
\begin{center}
\caption{Daten der Fahrzyklen ECE, EUDC, NEFZ.}\vspace{1ex}
\label{tab:tabnefz}
\begin{tabular}{l|ccc}
\hline
Kennzahl & Einheit & ECE & EUDC & NEFZ \\
\hline
Dauer & s & 780 & 400 & 1180 \\
Distanz & km & 4.052 & 6.955 & 11.007 \\
Durchschnittsgeschwindigkeit & km/h & 18.7 & 62.6 & 33.6 \\
Leerlaufanteil & \% & 36 & 10 & 27 \\
\hline
\end{tabular}
\end{center}
\end{table}
```

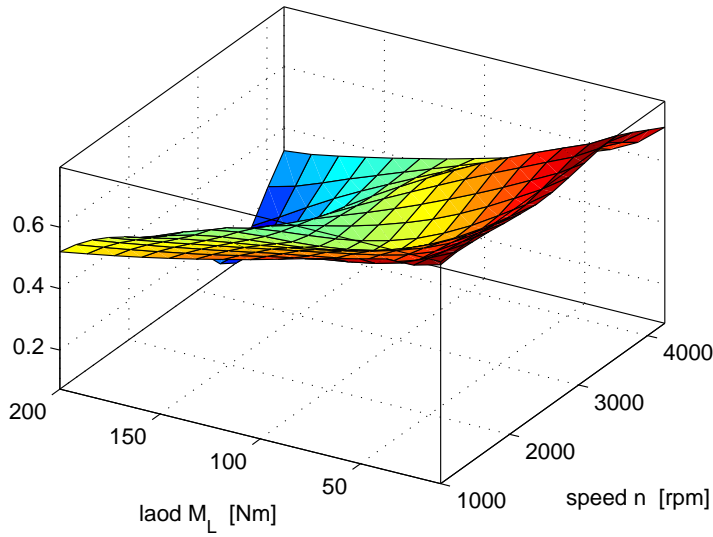


Figure 9.1: Ein Bild

9.5 Einbinden einer Grafik

Das Einbinden von Graphiken kann wie folgt bewerkstelligt werden:

```
\begin{figure}
  \centering
  \includegraphics[width=0.75\textwidth]{images/k_surf.pdf}
  \caption{Ein Bild.}
  \label{fig:k_surf}
\end{figure}
```

oder bei zwei Bildern nebeneinander mit:

```
\begin{figure}
  \begin{minipage}[t]{0.48\textwidth}
    \includegraphics[width = \textwidth]{images/cycle_we.pdf}
  \end{minipage}
  \hfill
  \begin{minipage}[t]{0.48\textwidth}
    \includegraphics[width = \textwidth]{images/cycle_ml.pdf}
  \end{minipage}
  \caption{Zwei Bilder nebeneinander.}
  \label{pics:cycle}
\end{figure}
```

9.6 Mathematische Formeln

Einfache mathematische Formeln werden mit der equation-Umgebung erzeugt:

$$p_{me0f}(T_e, \omega_e) = k_1(T_e) \cdot (k_2 + k_3 S^2 \omega_e^2) \cdot \Pi_{\max} \cdot \sqrt{\frac{k_4}{B}}. \quad (9.1)$$

Der Code dazu lautet:

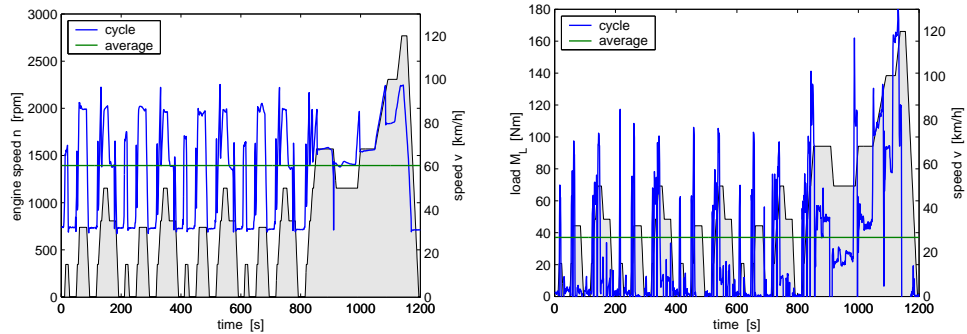


Figure 9.2: Zwei Bilder nebeneinander

```
\begin{equation}
p_{\text{meOf}}(T_e, \omega_e) = k_1(T_e) \cdot (k_2 + k_3 S^2 \cdot \omega_e^2) \cdot \Pi_{\text{max}} \cdot \sqrt{\frac{k_4}{B}}, .
\end{equation}
```

Mathematische Ausdrücke im Text werden mit \$formel\$ erzeugt (z.B.: $a^2+b^2=c^2$). Vektoren und Matrizen werden mit den Befehlen `\vec{.}` und `\mat{.}` erzeugt (z.B. \mathbf{v} , \mathbf{M}).

9.7 Weitere nützliche Befehle

Hervorhebungen im Text sehen so aus: *hervorgehoben*. Erzeugt werden sie mit dem `\textbf{emph}{.}` Befehl.

Einheiten werden mit den Befehlen `\unit[1]{m}` (z.B. 1 m) und `\unitfrac[1]{m}{s}` (z.B. 1 m/s) gesetzt.

Bibliography

- [] N. Hogan, “Impedance control: An approach to manipulation: Part ii—implementation,” *Journal of dynamic systems, measurement, and control*, vol. 107, no. 1, pp. 8–16, 1985.
- [1] P. Fiorini and Z. Shiller, “Motion planning in dynamic environments using velocity obstacles,” *The International Journal of Robotics Research*, vol. 17, no. 7, pp. 760–772, 1998.
- [2] D. Fox, W. Burgard, and S. Thrun, “The dynamic window approach to collision avoidance,” *IEEE Robotics & Automation Magazine*, vol. 4, no. 1, pp. 23–33, 1997.
- [3] R. Siegwart, I. R. Nourbakhsh, and D. Scaramuzza, “Autonomous mobile robots,” *Massachusetts Institute of Technology*, 2004.

Appendix A

Code

Appendix B

Datasheets

EC-max 30 Ø30 mm, brushless, 60 Watt

Part Numbers

	272762	272763	272764	272765

Motor Data

Values at nominal voltage	12	24	36	48
1 Nominal voltage V	12	24	36	48
2 No load speed rpm	7980	9340	9490	9350
3 No load current mA	302	191	130	95.4
4 Nominal speed rpm	6590	8040	8270	8130
5 Nominal torque (max. continuous torque) mNm	63.6	60.7	63.7	64.1
6 Nominal current (max. continuous current) A	4.72	2.66	1.88	1.4
7 Stall torque mNm	381	458	522	519
8 Starting current A	26.8	18.8	14.5	10.7
9 Max. efficiency %	80	81	82	82

Characteristics

10 Terminal resistance phase to phase Ω	0.447	1.27	2.48	4.49
11 Terminal inductance phase to phase mH	0.049	0.143	0.312	0.573
12 Torque constant mNm/A	14.2	24.3	35.9	48.6
13 Speed constant rpm/V	672	393	266	197
14 Speed/torque gradient rpm/mNm	21.2	20.6	18.4	18.2
15 Mechanical time constant ms	4.86	4.73	4.21	4.17
16 Rotor inertia gcm²	21.9	21.9	21.9	21.9

Specifications

Thermal data	17 Thermal resistance housing-ambient 7.4 K/W
	18 Thermal resistance winding-housing 0.5 K/W
	19 Thermal time constant winding 2.76 s
	20 Thermal time constant motor 1000 s
	21 Ambient temperature 1000 s
	22 Max. permissible winding temperature -40...+100°C
	+155°C
Mechanical data (preloaded ball bearings)	23 Max. permissible speed 15000 rpm
	24 Axial play at axial load < 6.0 N 0 mm
	> 6.0 N 0.14 mm
	25 Radial play preloaded
	26 Max. axial load (dynamic) 5 N
	27 Max. force for press fits (static) 98 N
	(static, shaft supported) 1300 N
	28 Max. radial loading, 5 mm from flange 25 N
Other specifications	29 Number of pole pairs 1
	30 Number of phases 3
	31 Weight of motor 305 g

Values listed in the table are nominal.

Connection motor (Cable AWG 20)

red	Motor winding 1	Pin 1
black	Motor winding 2	Pin 2
white	Motor winding 3	Pin 3
	N.C.	Pin 4

Connector Part number

Molex	39-01-2040
-------	------------

Connection Sensors (Cable AWG 26)

yellow	Hall sensor 1	Pin 1
brown	Hall sensor 2	Pin 2
grey	Hall sensor 3	Pin 3
blue	GND	Pin 4
green	V _{Hall} 3...24 VDC	Pin 5
	N.C.	Pin 6

Connector Part number

Molex	430-25-0600
-------	-------------

Wiring diagram for Hall sensors see p. 35

Operating Range

Comments

Continuous operation

In observation of above listed thermal resistance (lines 17 and 18) the maximum permissible winding temperature will be reached during continuous operation at 25°C ambient.
= Thermal limit.

Short term operation

The motor may be briefly overloaded (recurring).

Assigned power rating

maxon Modular System

Overview on page 20 - 25

Encoder MR
500/1000 CPT,
3 channels
Page 302

Encoder HEDL 5540
500 CPT,
3 channels
Page 308

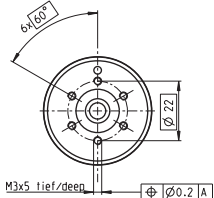
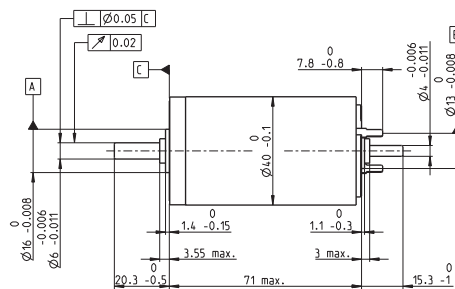
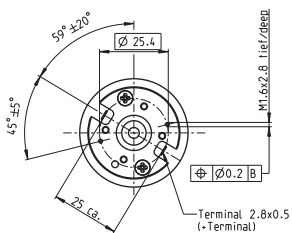
Brake AB 20
24 VDC
0.1 Nm
Page 346

Recommended Electronics:

ESCON 36/3 EC	Page 320
ESCON 50/5, Module 50/5	321
ESCON 70/10	321
DECS 50/5	324
DEC Module 24/2	325
DEC Module 50/5	325
EPOS2 24/5, 50/5	331
EPOS2 P 24/5	334
EPOS3 70/10 EtherCAT	337
Notes	24

June 2013 edition / subject to change

maxon EC motor 193

RE 40 Ø40 mm, Precious Metal Brushes, 25 Watt
NEW**maxon DC motor****M 1:2**

- Stock program
- Standard program
- Special program (on request)

Part Numbers

	448588	448589	448590	448591	448592	
Motor Data						
Values at nominal voltage						
1 Nominal voltage V	9	18	24	42	48	
2 No load speed rpm	2850	2850	2780	2920	2690	
3 No load current mA	49.7	24.8	18.1	11	8.62	
4 Nominal speed rpm	2610	2600	2480	2640	2410	
5 Nominal torque (max. continuous torque) mNm	87.8	87.8	88.2	87.6	87.6	
6 Nominal current (max. continuous current) A	2.96	1.48	1.09	0.65	0.524	
7 Stall torque mNm	873	956	794	895	818	
8 Starting current A	29	15.9	9.66	6.53	4.81	
9 Max. efficiency %	92	92	92	92	92	
Characteristics						
10 Terminal resistance Ω	0.311	1.14	2.49	6.43	9.97	
11 Terminal inductance mH	0.0824	0.33	0.613	1.7	2.62	
12 Torque constant mNm/A	30.2	60.3	82.2	137	170	
13 Speed constant rpm/V	317	158	116	69.7	56.2	
14 Speed / torque gradient rpm/mNm	3.27	2.98	3.51	3.27	3.3	
15 Mechanical time constant ms	4.85	4.29	4.36	4.14	4.13	
16 Rotor inertia gcm²	142	137	119	121	120	

Specifications**Thermal data**

17 Thermal resistance housing-ambient	4.65 K/W
18 Thermal resistance winding-housing	1.93 K/W
19 Thermal time constant winding	41.5 s
20 Thermal time constant motor	809 s
21 Ambient temperature	-20...+85°C
22 Max. permissible winding temperature	+100°C

Mechanical data (ball bearings)

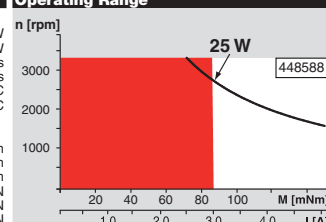
23 Max. permissible speed	3330 rpm
24 Axial play	0.05 - 0.15 mm
25 Radial play	0.025 mm
26 Max. axial load (dynamic)	5.6 N
27 Max. force for press fits (static)	110 N
(static, shaft supported)	1200 N
28 Max. radial loading, 5 mm from flange	28 N

Other specifications

29 Number of pole pairs	1
30 Number of commutator segments	13
31 Weight of motor	480 g

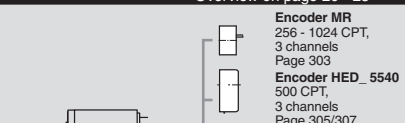
Values listed in the table are nominal.
Explanation of the figures on page 71.

Option
Preloaded ball bearings

Operating Range**Comments**

■ **Continuous operation**
In observation of above listed thermal resistance (lines 17 and 18) the maximum permissible winding temperature will be reached during continuous operation at 25°C ambient.
= Thermal limit.

■ **Short term operation**
The motor may be briefly overloaded (recurring).

Assigned power rating**maxon Modular System****Overview on page 20 - 25****Recommended Electronics:**

ESCON 36/2 DC	Page 320
ESCON 50/5	321
ESCON Module 50/5	321
EPOS2 24/2	330
EPOS2 Module 36/2	330
EPOS2 24/5	331
EPOS2 50/5	331
EPOS2 P 24/5	334
EPOS3 70/10 EtherCAT	337

Notes

22

maxon DC motor